ORIGINAL ARTICLE

CIWEM Chartered Institution of Water and Environmental Management | Journal of Flood Risk Management | **WILEY**

Flood vulnerability and risk assessment of historic urban areas: Vulnerability evaluation, derivation of depth-damage curves and cost–benefit analysis of flood adaptation measures applied to the historic city centre of Tomar, Portugal

Lucy Davis[1,2] | Tatiana Larionova[1] | Dhairya Patel[1] | Demiana Tse[1] | Pilar Baquedano Juliá[1] | Pedro Pinto Santos[3] | Tiago Miguel Ferreira[4]

[1]ISISE, Department of Civil Engineering, University of Minho, Guimarães, Portugal

[2]Department of Civil Engineering, McGill University, Montréal, Canada

[3]Centre for Geographical Studies, Institute of Geography and Spatial Planning (IGOT), Associated Laboratory TERRA, University of Lisbon, Lisbon, Portugal

[4]School of Engineering, College of Arts, Technology and Environment (CATE), University of the West of England (UWE Bristol), Bristol, UK

Correspondence
Tiago Miguel Ferreira, School of Engineering, College of Arts, Technology and Environment, University of the West of England (UWE Bristol), Bristol, UK.
Email: Tiago.Ferreira@uwe.ac.uk

Abstract

Around 45% of natural hazards reported worldwide are related to floods, and current indications show that exposure to floods and inherent losses will keep escalating. Historic centres are particularly vulnerable in this context due to the structural and material characteristics of the buildings and because they embrace social and cultural values that must be safeguarded. This article aims to contribute to this research area by presenting and discussing the application of an index-based methodology specifically tailored to assess flood risk in historic urban centres. The historic city centre of Tomar, Portugal, an area that encompasses over 500 buildings and has a rich history of floods, is used here as a case study. Vulnerability data resulting from the application of the vulnerability assessment approach are then combined with flood hazard—that is, water velocity and depth obtained from flood peaks estimated for 20- and 100-year periods of return—and used to identify the buildings at risk. Finally, a set of depth-damage curves is derived and used here to carry out a cost–benefit analysis for different flood adaptation measures.

KEYWORDS
exposure, flood risk, historic urban centres, sensitivity, vulnerability assessment

1 | INTRODUCTION

Every year the world faces many climate-related and geophysical hazards. And although low-income countries tend to be particularly affected by those hazards due to poor infrastructure systems, disastrous floods in countries like Pakistan, Puerto Rico, the United States, and the United Kingdom prove that floods are a global threat (Rentschler et al., 2022). In Europe alone, reported economic losses due to disasters amount to 281 billion US$, of which 52% are due to floods. It is estimated that exposure to floods, and consequently damage losses, will grow

by a factor of three by 2050 due to increases in population and economic assets in flood-prone areas (Merz et al., 2021).

Climate change has become one of the most important concerns for cultural heritage sites (UNESCO-WHC, 2021). The Sendai Framework 2015–2030 (UN, 2015) and the 2030 Agenda for Sustainable Development (UN, 2018) clearly mention the need to strengthen efforts to protect cultural and natural heritage as a key point to increase the resilience of communities. Furthermore, various international organisations have highlighted the urgency of taking action through the development of documentation and projects supporting preventive, operational and resilience measures aimed at the reduction and mitigation of damage and losses caused by natural hazards (Bonazza et al., 2018; Jigyasu, 2016; Jigyasu et al., 2013; UNESCO et al., 2010; UNESCO; UNEP, 2016; UNESCO-WHC, 2008, 2021).

Despite these efforts, flood events have had a significant impact on cultural heritage and historic centres in recent years (Holicky & Sykora, 2010; Lanza, 2003; Vojinovic et al., 2016), and the trend continues to increase. A recent study analysing 1121 sites as of March 2021 shows that 35% of natural and 21% of cultural and mixed UNESCO Tangible World Heritage sites are in geographical areas that are likely to be affected by flood hazards (Arrighi, 2021). This represents a significant threat since these assets combine high cultural value with a series of characteristics that make them potentially vulnerable to physical, chemical, and biological degradation because of moisture ingress (Sesana et al., 2021; Stephenson & D'Ayala, 2014). It is worth clarifying in this point that, in the context of the present article, vulnerability encompasses exposure and sensitivity and is understood as the intrinsic predisposition of the buildings to suffer damage from a flood event—further details on this are provided in Section 3. It is also important to state that, despite the high level of scholarly interest in assessing the impacts of climate change, a comprehensive understanding of the impacts of floods on cultural heritage buildings is still notably absent from the literature (Fatorić & Seekamp, 2017).

The present article attempts to fill that gap through the application of a large-scale risk assessment of the historical city centre of Tomar. Founded in the 12th century, this city has historically been strategically important in Portugal for a long time, and its history is closely associated with the Knights Templar. Due to its proximity to the river, the city centre has been affected by at least 14 floods from 1852 to 2019, which, together with its great historical value, justifies its choice as the subject of this large-scale risk assessment. This analysis involved quantifying the vulnerability of the buildings using a simplified approach based on indices and then overlaying that vulnerability with hazard scenarios obtained for two different return periods (20 and 100 years) to estimate the level of risk associated with each building. Finally, some flood adaptation measures were analysed in the context of a cost–benefit analysis performed from a set of original flood vulnerability curves. With this article, the authors hope to offer a valid contribution to consolidating the knowledge in different areas, including (i) the design of field matrices for the physical vulnerability of buildings; (ii) the relationship between the expected damage on buildings following a particular hazard scenario; and (iii) the theoretical benefits of common retrofitting measures tailored to the type of building.

2 | THE CITY OF TOMAR

The municipality of Tomar is in the geographical centre of Portugal, in the Santarém District of Ribatejo Province. It has a population of 40,677 inhabitants in an area of 351.2 km^2. The city is divided by the Nabão River into two zones: the historical centre and the new part of the city (Câmara Municipal de Tomar, 2021).

Even though human settlement can be dated back to more than 30,000 years ago, the city's developmental history is closely related to the history of the Knights Templar. In 1159, the land was granted to the Order of Templar Knights. The first stone of the castle and Convent of the Knights Templar was laid by Gualdim Pais in 1160. In the 14th century, the town of Tomar experienced significant growth. In the Várzea Pequena area, an orthogonal city planning was applied, according to which the development was perpendicular to the river. Between the mid-17th century and the end of the 19th century, Tomar underwent significant industrial development. In the 1950s, the Castelo do Bode hydroelectric dam was inaugurated, becoming, at that time and for the following 50 years, the largest dam in the country. In 1983, UNESCO recognised the Castelo Templário-Convento de Cristo complex as a World Heritage Site, and in the early 1990s, the first steps were taken towards the restoration and consolidation of the historic centre.

The historic city centre of Tomar and the region around it are prone to flooding due to its proximity to the Nabão River. The Nabão river basin (1053 km^2) is part of the Zêzere river basin (5043 km^2), which is one of the main affluents of the Tejo River (22,822 km^2 in Portugal). The history of flooding caused by the Nabão River is mainly reported in the urban area of Tomar since the urban area is divided by the river (Rodrigues, 2017). There are reports of 14 floods that have affected the historic city centre of Tomar (FBO Consultores, 2003). Some

photos of events documented throughout the history of the city can be seen in Figure 1.

3 | CONCEPTUAL FRAMEWORK OF THE FLOOD RISK ASSESSMENT METHODOLOGY

The flood risk assessment methodology adopted in this study is composed of two components—a hazard and a vulnerability component, as illustrated in Figure 2 for better understanding. The bases of each of those are explained in Sections 3.1 and 3.2, respectively. However, roughly speaking, the hazard was assessed based on water depth and velocity results obtained using a 2D hydrodynamic model. The flood vulnerability, in turn, was broken down into two sets of vulnerability factors, one related to the sensitivity of the building to flood water and the other related to its exposure. It is worth

noting that, in the context of this work, exposure is measuring the likelihood and significance of the losses that may result from the exposure of the building, as a singular entity, to a flood, given the characteristics of the immediate setting of the building, and its economic and heritage value. The results obtained from these two components were then integrated and mapped with the help of a GIS tool, which was also used to represent the level of flood risk associated with each building in the historic city centre of Tomar. As detailed in Section 3.3, flood risk was computed here from the combination of the hazard and the vulnerability results by using a flood risk matrix. All these results were finally used to estimate losses and perform a cost–benefit analysis where the potential impact of some flood adaptation measures was investigated; refer to Section 5. For such, the damage-depth curves developed by Martínez-Gomariz et al. (2020) for the city of Barcelona, Spain, were used in this work as a basis to derive a set of flood vulnerability curves adapted

FIGURE 1 Flooding in the city centre: (a) 1915–1931 Rua Everard; (b) 1950–1957, Praceta Alves Redol. *Source*: (Memória Digital de Thomar, 2013).

(a)   (b)
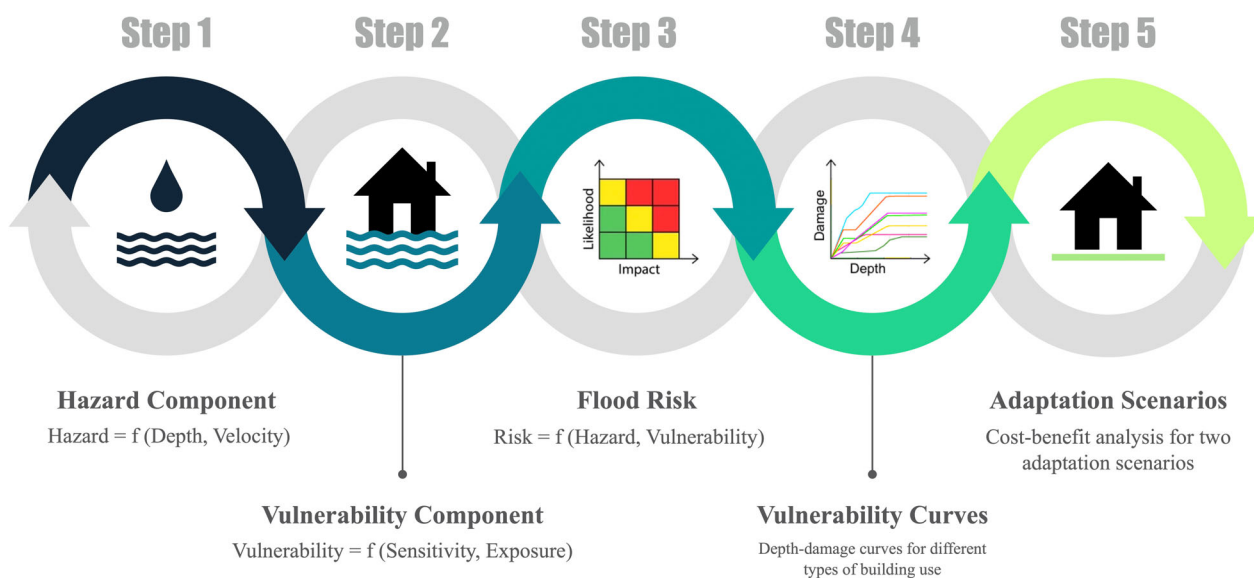
FIGURE 2 The conceptual framework of flood risk assessment methodology.

to the specific characteristics of the buildings in the Tomar. Such a process involved converting the relative damage into economic damage per square metre ($€/m^2$) with an adjustment factor calculated from regional price indicators ratios compared to those for Barcelona. The adjustment factor used was 0.215 based on the historical sales price difference between Tomar and Barcelona (Historical sales prices Tomar and Santa Maria dos Olivais, 2021).

3.1 | Hazard component

The hazard component of the flood risk assessment is based on the hydrologic and hydraulic models developed by the Portuguese Environmental Agency (Brandão et al., 2014) under the scope of the implementation of the European Union Floods Directive. Flood hazard extent, depths and velocities were later evaluated and processed in collaboration with the Institute of Geography and Spatial Planning at the University of Lisbon. In our study, the flood velocities and depths for the 20-year and 100-year return periods were used, associated respectively with frequent, rare, and exceptional flooding events.

On the hydrologic component of the hazard model, a first probabilistic and statistical approach was applied, followed by a physically-based model that simulates the rainfall-runoff relationship, resulting in the flood hydrographs for the two return periods. The probabilistic model examined the annual instantaneous maximum discharge (m^3/s) of two-gauge stations, Agroal and Fábrica da Matrena, which are located upstream and downstream, respectively, from Tomar. The second analysis consisted of validating the first analysis with a hydrologic model made for the Nabão river using the MOHID Studio software, which implements the MOHID Land model. The MOHID Studio software found that the hydrologic model outputted values that were 11%–23% of the ones obtained using the statistical model analysis. After, comparisons to previous studies were conducted using the Hydrologic Engineering Center-Hydrologic Modelling System (HEC-HMS). Since the comparisons were consistent, the hydrologic model created for the Nabão was considered valid. On the hydraulic component of the hazard model, the 2D hydraulic MOHID Land and MOHID Water models were run within the MOHID Studio environment using the flood hydrographs previously estimated. The 2D momentum and mass conservation equations were solved upon a finite element mesh, created with a 10 m × 10 m cell size, based on 1:10,000 scale maps. The resulting flood depth and velocity mapping were compared with the data obtained from the field survey to establish which buildings have the greatest risk of flooding in Tomar.

3.2 | Vulnerability component

Estimating damage losses from future flooding is essential for disaster preparedness, as it provides a basis for decision-makers for urban planning, development of risk reduction policies and evaluation of the cost-effectiveness of approaches to strengthening disaster-mitigating measures (Dutta et al., 2001). A key factor in flood risk assessment and damage loss estimation is the assessment of the vulnerability of the elements at risk (Velasco et al., 2016). A variety of approaches have been developed to assess vulnerability (Huang et al., 2012; Nasiri et al., 2016). However, index-based assessment approaches are particularly suitable for conducting flood vulnerability assessment in urban areas as they allow for generalised visibility of vulnerability in a given space through a transparent process and enable the integration of different dimensions of vulnerability, which vary according to the objective (emergency management or mitigation and preparedness activities) and the scale of the approach.

In the last decade, different index-based methods have been developed to assess flood vulnerability in historic city centres—see, for example, those developed by Gandini et al. (2018), Mebarki et al. (2012), Miranda and Ferreira (2019), and Stephenson and D'Ayala (2014), all recently analysed by Baquedano Juliá and Ferreira (2021). Most methodologies incorporate parameters of physical, socio-economic and cultural vulnerability dimensions of the building, with the exception of the methodology presented by Mebarki et al. (2012), which is only focused on assessing physical vulnerability. From the individual parameters used by Mebarki et al. (2012) and Stephenson and D'Ayala (2014), Miranda and Ferreira (2019) propose the assessment of a Flood Vulnerability Index (FVI) based on the development of composite indices related to sensitivity (SC) and exposure (EC). The main advantage of using composite indicators is that they can summarise complex and multidimensional realities in order to support decision-makers. Moreover, they can be easier to interpret than a battery of separate indices (Saisana & Tarantola, 2002).

This study presents an extended version of the Flood Vulnerability Index (FVI) method, initially developed by Miranda and Ferreira (2019) and subsequently applied by Ferreira and Santos (2020). The proposed method is based on the calculation of the vulnerability index considering a total of 10 parameters (see Table 1), which were defined based on similar indicators already available in the literature, developed for assessing analogous building typologies and structural characteristics under equivalent assessment conditions. The sensitivity component (SC) is comprised of seven parameters that encompass the physical state of the building stock. The exposure component (EC) consists of three parameters

TABLE 1 Flood vulnerability index: parameters, classes and weights.

Components	Parameters	Attributes	Class C_{vi}	Weight p_i
Sensitivity	S1—State of conservation	No damage/cracking	A	10
		Slight cracking (under 0.5 mm)/moisture	B	40
		Generalised cracking (around 2–3 mm)/settlements/erosion	C	70
		Deformation/serious material decay	D	100
	S2—Structural material	Reinforced concrete/steel structures	A	10
		Masonry structures	B	40
		Timber structures	C	70
		Earth structures	D	100
	S3—Finishing material of the facades	Steel/concrete/glazed tile/glass	A	10
		Brick/plaster/regular dressed stone	B	40
		Unglazed tile/irregular stone/wood panels	C	70
		Earth/rubble stone	D	100
	S4—Type and condition of window/door frames	Plastics	A	10
		Metals	B	40
		Wood	C	70
		Total exposure	D	100
	S5—Openings at ground floor	Without openings	A	10
		Window openings, without door openings	B	40
		Window and door openings	C	70
		Large openings	D	100
	S6—Existence of basements	No basement	A	10
		Basement without windows; no direct access	B	40
		Basement with windows; no direct access	C	70
		Basement with direct access	D	100
	S7—Height of the door threshold	2 or more steps	A	10
		<2 steps	B	40
		Level with the outside	C	70
		Down 1 or more steps	D	100
Exposure	E1—Type of use or activity	Educational/dwelling	A	10
		Commercial	B	40
		Restaurant	C	70
		Hotel/religious	D	100
	E2—Surface condition	Convex	A	10
		Flat and permeable	B	40
		Flat and impermeable	C	70
		Concave	D	100
	E3—Heritage value	Non-classified buildings	A	10
		Non-classified buildings of high public interest	B	40
		Buildings of national or local interest	C	70
		Buildings of international interest	D	100

describing the unprotectedness of the building based on its orientation, the use of the building, and its heritage value. Each parameter is defined by four classes (A, B, C, D) that rank the vulnerability from lowest to highest with a certain weight. A (10), B (40), C (70) and D (100). The scale starts at 10, as it was assumed historic buildings will always have some degree of vulnerability to flooding (Stephenson & D'Ayala, 2014).

### 3.2.1 | Sensitivity parameters

The sensitivity component consists of seven parameters aimed at identifying the physical characteristics of the building and the possibility of its envelope being affected by flooding. The state of conservation (S1) is defined by the condition assessment of the structure. The poor condition of the structures reduces their resistance to flood loads and increases the possibility of water infiltration, aspects which can cause physical losses (Stephenson & D'Ayala, 2014). The classes were defined mainly according to the criteria described by Miranda and Ferreira (2019). Structural material (S2) parameter evaluates the ability of the material to be damaged and deteriorated by water due to its porosity and surface characteristics, whereas the finishing material of the facades (S3) evaluates the main cladding of the building, which acts as the first barrier to water. Different materials will have different behaviours in the short term with respect to water exposure. Higher sensitivity is seen in materials with a greater porosity and those that are more sensitive to degradation (Gandini et al., 2020).

The remaining four sensitivity parameters are related to the physical characteristics of the building openings and the possibility of water entering the building and damaging its contents. The sensitivity class to the type and condition of opening frames (S4) were determined based on existing research into the ability of the finishing materials of the building, including windows and doors, to resist flood water damage (FEMA, 2008). The openings at the ground floor parameter (S5) are used to evaluate the possibility of water infiltration through the windows and doors. A larger number of openings increases the sensitivity class of the building (Gandini et al., 2020). The

existence of basements (S6) increases the sensitivity of buildings to floods, as it is the most sensitive part of the buildings to flooding (Gandini et al., 2020; Martínez-Gomariz et al., 2021). The presence of openings and direct access from outside into the basement further increases the risk of water infiltration into the building. Finally, the height of the door threshold (S7) is determined from the plinth. An increase of multiple steps from the plinth to the door threshold would reduce the sensitivity class of the building. Consequently, if the door threshold is below the plinth, this would increase the sensitivity class (D'Ayala et al., 2020; Martínez-Gomariz et al., 2021).

3.2.2 | Exposure parameters

The exposure component is composed of three parameters, which help to identify the likelihood of economic, physical, and cultural damage or loss. Floods not only physically damage assets but also suspend economic activity and may compromise the attributes that underpin their cultural value. The type of use or activity parameter (E1) describes the potential economic losses from flooding that a property may suffer with respect to the type of use. A building will have a higher or lower exposure to flood damage based on the type of use or activity within the building. To determine the exposure class of a type of property, the average relative damage of multiple types of properties was compared based on pre-existing tables (Martínez-Gomariz et al., 2020). As mentioned before, the surface condition (E2) assesses the characteristics of the immediate setting of the building, including the inclination of the ground—whether the ground in the vicinity of the buildings has positive, negative or no concavity (i.e., whether it is convex, concave, or flat)—and its permeability (see Figure 3). A concave ground will decrease the exposure of the building since the water will tend to flow off the building. On the other hand, a concave ground will retain the water in the vicinity of the building, increasing its exposure. Flat ground can be considered neutral concerning this aspect. Additionally, the permeability of the ground refers to the existence of drainage systems in the vicinity of the building

(a)   (b)   (c)   (d)
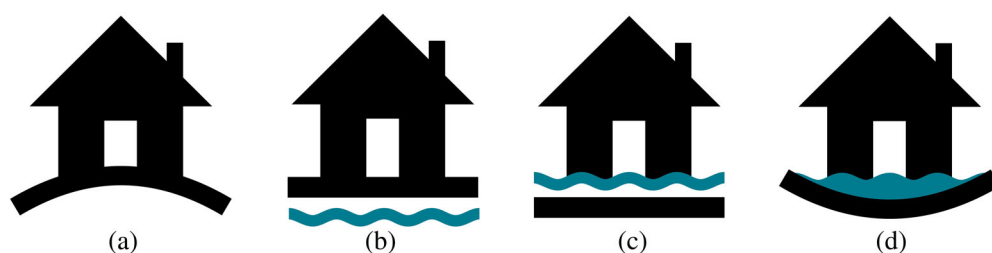
FIGURE 3 Exposure classes of Parameter E2, surface condition: (a) convex; (b) flat and permeable; (c) flat and impermeable; and (d) concave.

(D'Ayala et al., 2020). Finally, the potential cultural value of the building is considered through Parameter E3, heritage value. This parameter is aimed to incorporate the cultural value of the building and, in that way, the potential cultural impact resulting from its damage and loss of value (Miranda & Ferreira, 2019).

3.3 | Risk analysis

Flood hazard and vulnerability were aggregated here using a risk matrix. In agreement with the current climate change adaptation literature, the vulnerability of each building is determined using a Flood Vulnerability Index (FVI) given by Equation (1).

$$
\begin{aligned}
&\text{Flood Vulnerability Index(FVI)} \\
&= \text{Exposure Index(EI)} \times \text{Sensitivity Index(SI)}.
\end{aligned} \tag{1}
$$

Once the FVI is determined, the vulnerability of the buildings can be divided into four categories. Each category is obtained by redistributing the results of the FVI according to the mean. In this way, the values can be redistributed over the entire range of the vulnerability results. The four categories (low, moderate, high and extreme) are divided according to the criteria proposed by Rana and Routray (2016). The results from the hazard analysis were redistributed into five levels based on the classes of hazard as defined in the Portuguese Floods Directive; Equation (2) and Table 2.

$$
\text{Flood Hazard Index (FHI)} = \text{Depth} \times (\text{Velocity} + 0.5). \tag{2}
$$

The depth and velocity values at each building are the maximum values found within their implantation limit. The percentage of the buildings' area was also considered as a factor applied to the previous hazard score. With the distributed values of vulnerability and hazard, the result

can be plotted into a matrix to determine the flood risk Table 2. The final flood risks are reported and analysed in the results.

3.4 | Study area, inspection procedure and database

As mentioned before, this research focuses on the old area of the city centre of Tomar. With a total area of approximately 100,000 m², it is composed of 520 buildings, most of them low-rise buildings, divided into irregular blocks forming a grid system. To improve the efficiency of the fieldwork and organise the information in a systematic and logical way, the process of data collection followed the 'Site Approach' methodology proposed by Granda and Ferreira (2019). According to this data collection approach, the fieldwork is organised around three fundamental axes, 'site context', 'urban development', and 'building characterisation': the first axis is related to the gathering of relevant information about the study area, the second one is about gathering and studying historical information about the evolution of the site, whereas the third one is about the identification of the features that rule the vulnerability of the buildings. Together, these sets of data allow for a comprehensive overview of the study area, not only regarding its current state but also about the factors that have contributed to that state. Finally, QGIS Software was used to store, manage, analyse and map the information collected during the survey. Due to the large amount of data collected and time restrictions on site, the Input application was used to streamline and speed up the field survey. The Mergin plugin, which acted as the database coordinator, allowed one to access the maps and parameters fields on smartphones using the previously mentioned Input application. Once the information was collected, it was synchronised with the cloud to ensure that the information was safely stored in QGIS. After that, the information collected on the Input application would be able to

TABLE 2 Flood risk matrix.

Flood risk		Hazard level [FHI= Depth (velocity+ **0.5**)]				
		Negligible [H ≤ **0.5**]	**Low** [**0.75** < H ≤ **1.25**]	**Moderate** [**1.25** < H ≤ **2.5**]	**High** [**2.5** < H ≤ **7.0**]	**Extreme** [H > **7.0**]
Vulnerability level	Extreme [> Mean + SD]	Moderate	High	Extreme	Extreme	Extreme
	High [Mean to (Mean+ SD)]	Low	Moderate	High	Extreme	Extreme
	Moderate [(Mean− SD) to Mean]	Low	Low	Moderate	High	Extreme
	Low [< Mean − SD]	Negligible	Low	Low	Moderate	High

Note: The greens, yellow and reds are used to illustrate the different risk levels.

FIGURE 4 State of conservation (a) fully demolished, (b) bad state of conservation, and (c) good state of conservation.

be accessed using the QGIS software for further off-site analysis.

During the survey, it was found that many buildings had a similar typology. The majority of the buildings were unlisted residential or commercial buildings made of masonry in various states of conservation. Some buildings had been fully demolished (Figure 4a), others were in a bad state of conservation (Figure 4b), but the majority of them were in a good state of conservation or with slight cracking (Figure 4c).

4 | FLOOD RISK ASSESSMENT: RESULTS AND DISCUSSION

The most relevant results related to flood hazard, vulnerability and risk are given and discussed in the present section.

4.1 | Flood hazard

Peak flood discharges were found for 20-year and 100-year periods of the two-gauge stations Agroal (340 m³/s, 518 m³/s) and Fábrica da Matrena (626 m³/s, 973 m³/s). Despite such a difference in the flood peak flows between the two return periods, the mapping does not show a proportional extent between the two floodable areas. Three factors explain this: the wideness of the main channel and the height of its longitudinal banks, which accommodates a significant flood volume before full bank discharge is reached; the low roughness coefficients, which promote high velocities in the main

channel; and the overbank morphology, with flat areas contiguous to the main channel and intermediate embankments preventing a planar expansion of floodwaters to outer zones in the city. The peak discharges, as well as the depth and the velocity of the water during flooding, were used here to determine the hazard component for the flood risk of each building, mapped for each building polygon along with flood depth and velocity for return periods of 20-year and 100-year (Figure 5). The largest flood risk that occurred within the polygon of each building shows the buildings closest to the river will be completely affected by the flood, the southeast corner of the city.

4.2 | Flood vulnerability

The vulnerability of each of the buildings was determined using data from the survey completed. Using the parameter classification, the combination of the sensitivity and exposure components could be evaluated, as well as the FVI. First, the total sensitivity for each building was calculated and normalised within a range of 0–100. The statistical distribution of the dataset has a mean of 36.32 and a standard deviation of 7.02, as given in Figure 6a. The exposure class distribution, Figure 6b, is skewed to the left and has an average of 24.29 (STD = 12.66), likely due to the similar level heritage values (Parameter E3), which was of no heritage value.

Following this, the flood vulnerability index (FVI) was calculated using Equation (1). The FVI was normalised to be within the range of 0 and 100 and plotted on a histogram, Figure 6c, in order to check the distribution of
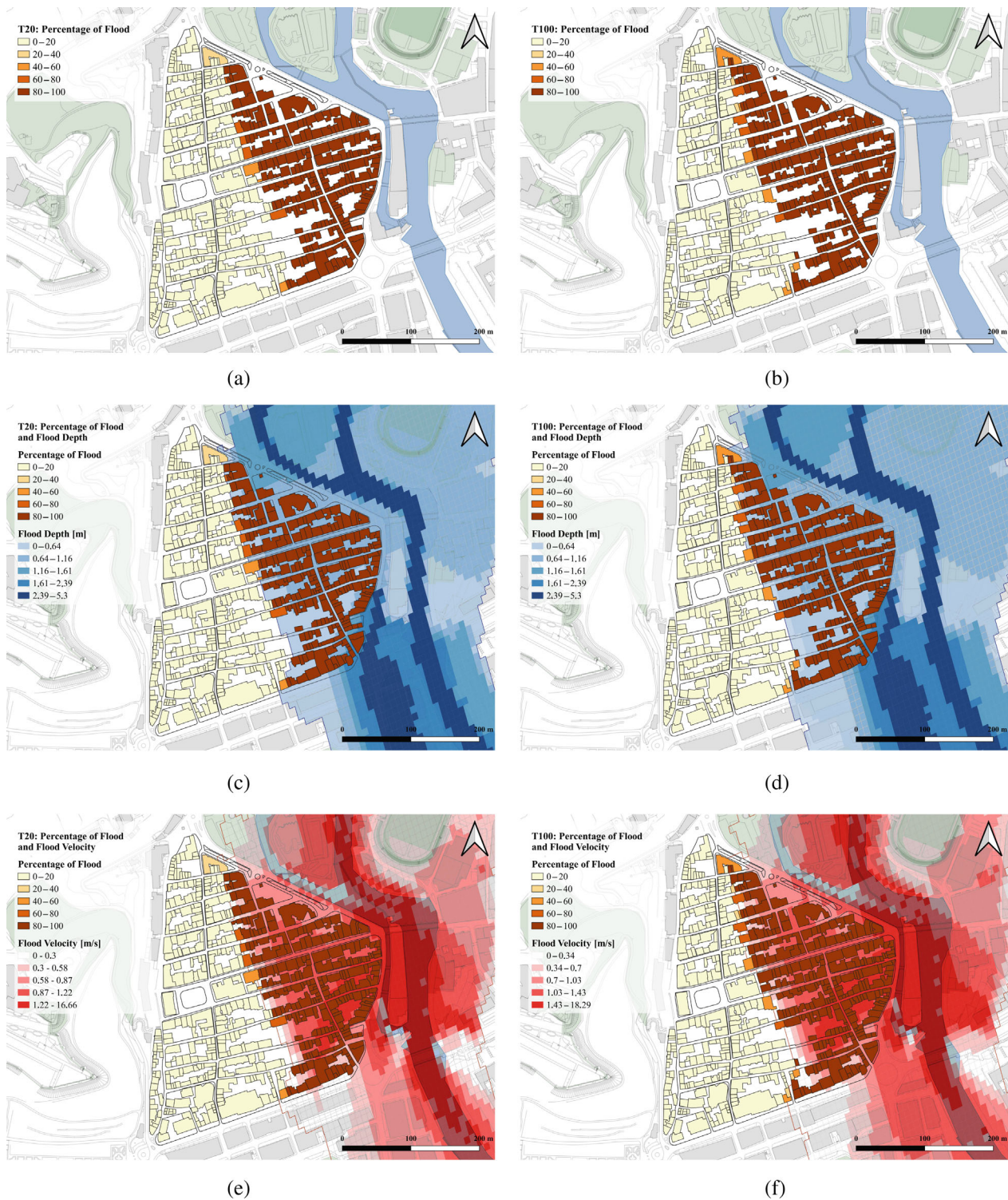
FIGURE 5 Percentage of the building's area overlaid with the flood-prone area with (a) 20-year return period and (b) 100-year return period (c, d) indicating flood depth and (e, f) flood velocity for 20 and 100-year return periods.

the results. The FVI ranges from 0 to 40, with a mean average of 12.79 and a standard deviation of 5.51. These values correspond to a low vulnerability to the risk of flooding events. Values of Low, Moderate, High, and Extreme were associated with each numerical value of

FVI, based on the previously defined risk analysis procedure, distributed in Figure 7.

Many of the buildings which had High or Extreme values were located along the major streets of the city centre, shown in Figure 8. Similarly, many buildings
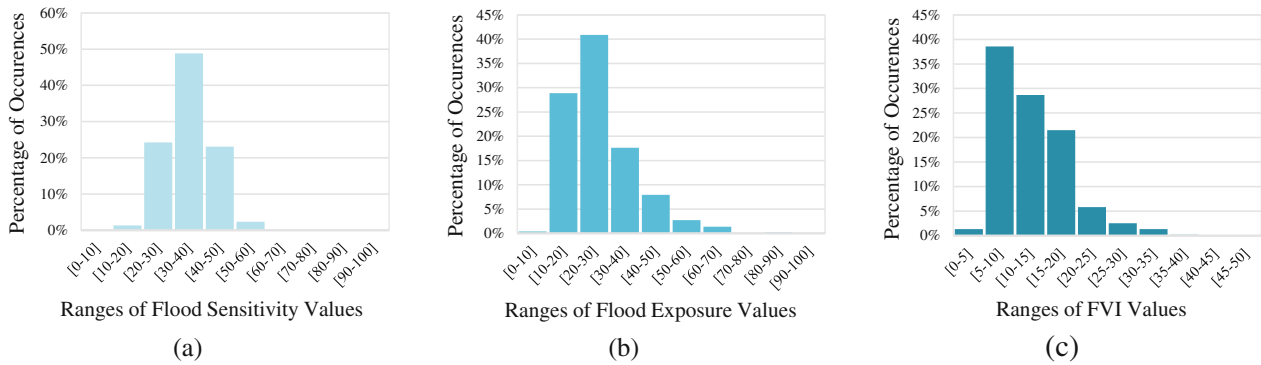
FIGURE 6 Histogram of the number of occurrences of (a) flood sensitivity values; (b) flood exposure values; and (c) flood vulnerability index values within a given range.
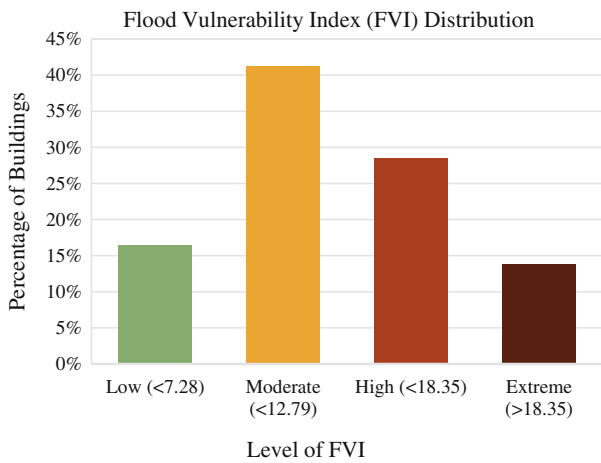

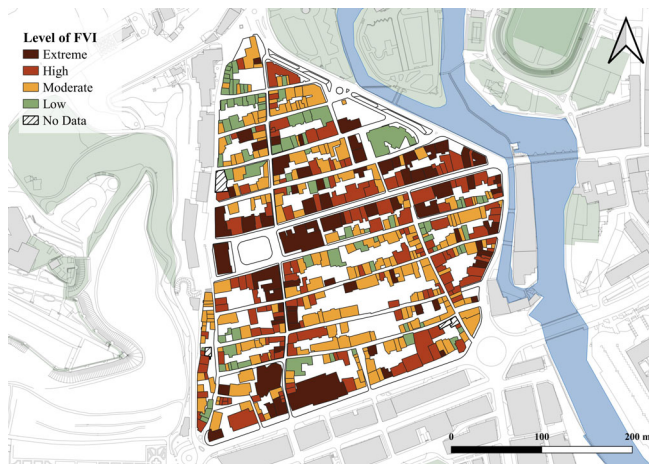**FIGURE 7** Flood vulnerability index distribution.

FIGURE 8 Flood vulnerability index values for each building.

surrounding the main plaza had FVI values of Extreme. The cause of this is likely due to the heritage value of the buildings. Furthermore, the buildings in the main plaza were not used for residential purposes on the ground level, which increased the FVI level, albeit being further from the hazard.

4.3 | Flood risk

A flood risk matrix for both the 20-year and 100-year return period floods was computed (Table 2). The flood risk per building can be seen in the maps in Figure 9. Flood risk for the 20-year and 100-year return periods is remarkably similar, with only a small increase of risk in the 100-year return period. Based on this analysis, the flood risk for the city of Tomar is relatively low. The buildings along the main street, as well as those on the closest street to the river, have a high number of buildings with an extreme risk of being affected by a flood event. It is also shown that the buildings most intersected by the extent of the flood are some of the more vulnerable ones. With respect to the level of risk, many of the buildings with moderate flood risk have got extreme FVI values. In many cases, this is associated with the heritage value of the buildings, particularly those surrounding the main plaza. It should be noted that a significant part of the buildings located in residential areas and outside of the hazard zone have either low or negligible levels of flood risk as a result of the level low or negligible level of hazard.

The following distribution shows more about the number of buildings in each category, as in Figure 10. The values of the flood risk from 20 to 100 years do not widely differ. Only 17 out of 512 buildings have an increased flood risk value when evaluating first the 20-year and then the 100-year flood risks. Additionally, 60% of the buildings have a negligible or low risk, and 81.8% have negligible, low, or moderate risk.

The results from this report can contribute to preparation for a flood event with respect to decisions on the most impactful changes to make. The ability to characterise the importance of different parameters contributing to the vulnerability of each building to flood is critical. In this specific case, the most concerning aspects were found to be the openings on the ground floor, the type of window and door frames and the building's concavity.
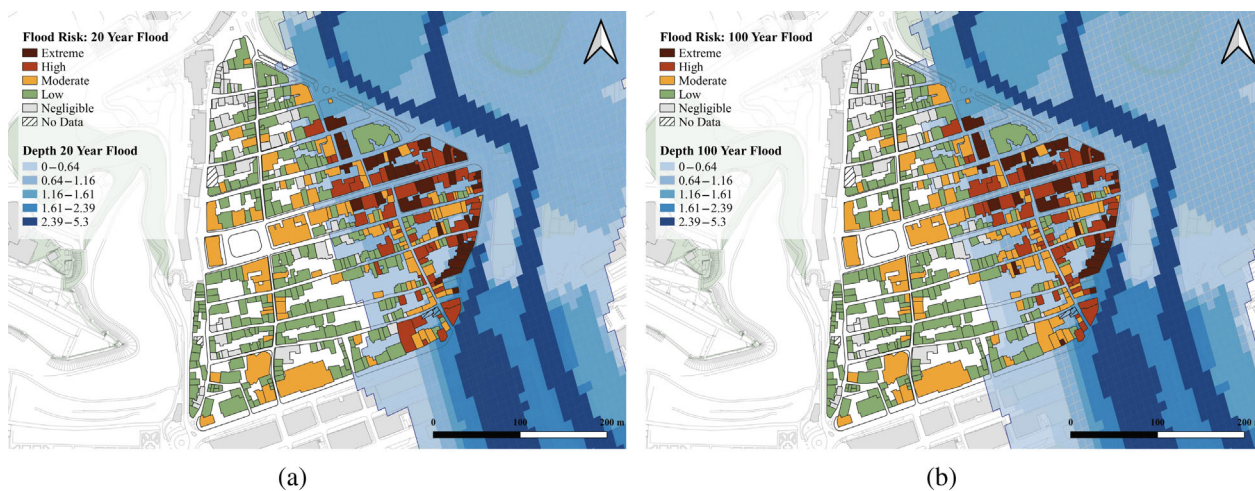
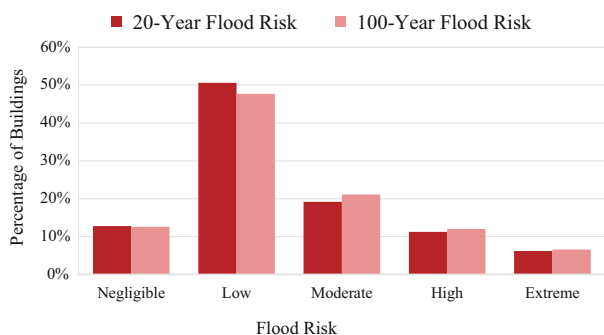**FIGURE 9** Flood risk per building for (a) 20-year return period and (b) 100-year return period.

FIGURE 10 Flood risk distribution.

FIGURE 11 Flood vulnerability curves for Tomar.

These parameters greatly impacted the sensitivity and exposure components.

5 | DEVELOPMENT OF FLOOD VULNERABILITY CURVES AND ESTIMATION OF ECONOMIC LOSSES

The flood risk curves given in Figure 11 shows that the economic damages created by flooding are maximised around 1.5 m flood depth. If the flood exceeds this depth, there are no further associated damages, except for workshops. The greatest depth of flooding faced by the buildings in Tomar (Figure 5c,d) is at a level of 2.5 m, by which time the associated economic damages will have been reached. Assuming that the depth-damage curves created for Barcelona follow a normal distribution, the depth-damage curves shown in Figure 11 are representative of buildings with a moderate level of vulnerability. In order to obtain representative economic damages, the curves can be modified according to the average level of flood risk in the city centre of Tomar.
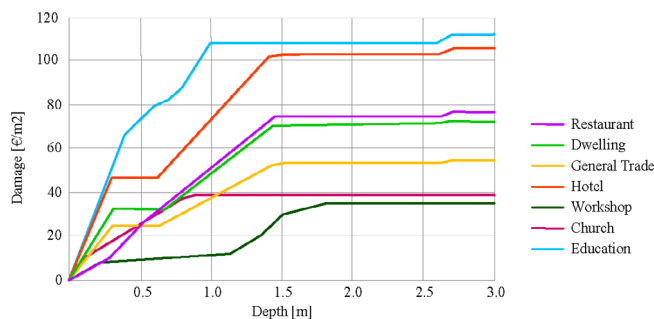
According to the flood risk results obtained in Section 4.3, the average flood risk level of the buildings in the Centre of Tomar is Low. Considering the central level of flood risk Low, an adjustment factor of the depth-damage curves was used to vertically shift the curves as, for example, buildings with an Extreme flood risk level will be more prone to damage, and the costs will be higher. The vertical adjustment of the curves reflects the costs according to the vulnerability of each building. Table 3 shows the average level of flood risk and the adjustment factor associated with each level. Finally, these factors can be applied to each building according to its level of flood risk, which is an update compared to simply assuming the values of the depth-damage curves shown in Figure 11.

Considering the use of the building (Parameter E1) and the cost as a function of the depth of flooding of the building multiplied by the area of the building, it was possible to obtain the total costs for the historic centre of Tomar (Table 4).

The cost distribution map can be seen in Figure 12. The greatest economic damage occurs in buildings used for education or housing due to their high cost per square metre of damage. Estimated the economic losses for the

TABLE 3 Average level of flood risk for depth damage curve and adjustment factors.

Flood risk level	Average level of flood risk	Adjustment factor
Negligible	13%	0.5
Low	51%	1
Moderate	19%	1.25
High	11%	1.5
Extreme	6%	1.75

TABLE 4 Economic damage in Tomar based on factored depth damage curves.

Building type	Cost (€)
Education or dwelling	1,127,800
Commercial	610,250
Restaurant	173,800
Hotel	81,100
Total	1,993,000
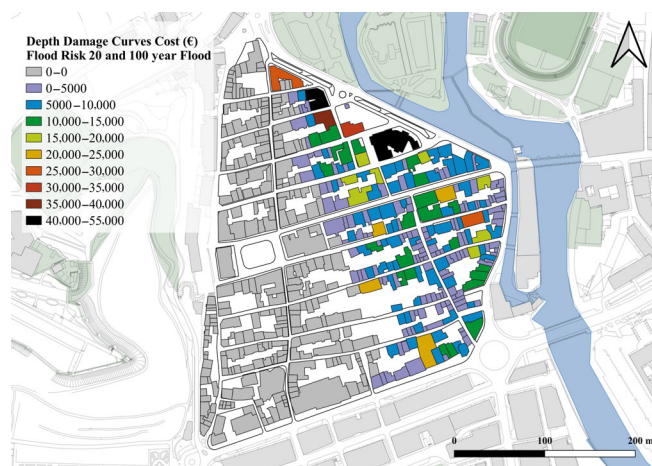
FIGURE 12 Depth-damage curves: Cost for 20- and 100-year flood risk.

different types of building use, the next step will involve the simulation of some flood adaptation measures and the analysis of the impact that those measures can have in terms of reducing the vulnerability of the buildings and, as a consequence of that, of the expected economic losses.

6 | INVESTIGATION OF POSSIBLE FLOOD ADAPTATION MEASURES

Flood adaptation measures are aimed at minimising the probability and the consequences of flooding events in

TABLE 5 Flood parameter mitigation techniques.

Parameter	Mitigation measure
S1: State of conservation	→ Fix plaster or repointing
S3: Finishing material of the facades	→ External render
S4: Type and condition of window/door frames	→ Change frame to metal or plastic
S5: Openings at the ground floor	→ Reduce number of openings, instal flood gates
E2: Concavity and permeability	→ Improve drainage systems

areas of high flood risk (Hegger et al., 2016; Xiao et al., 2021). Mitigation approaches can be divided into two categories, structural and non-structural. Structural mitigation strategies can be citywide or building-specific, while non-structural mitigation strategies deal with the removal of people and assets from areas of high flood risk during flooding events (Tyrrel, 2019). Two types of adaptation measures were investigated to assess the impact of implementing flood mitigation measures on a large scale—measures targeting the buildings, involving replastering and repointing, repairing external render, replacing doors and windows frames with metal or plastic frames, decreasing the number of openings and installing flood gates; and measures aimed at improving the capacity of the drainage system. By updating the parameters in the flood risk assessment based on the mitigation techniques shown in Table 5, the impact of these mitigation techniques could be measured.

In each analysis, the parameters were updated to a lower class, one that would make sense based on the type of mitigation measure applied. The updates are summarised in Table 6.

The first adaptation scenario involved updating the most critical buildings for each category (Class D). The second adaptation scenario was chosen to describe a more widespread measure that impacted many more buildings and should have a greater impact on the final flood risk (Class D and C).

6.1 | Vulnerability and risk reduction for the two adaptation scenarios

The results presented below result from the cumulative impact of each parameter if they were all updated in a citywide rehabilitation effort. First, the impact on the FVI can be seen in Figure 13. For adaptation scenario 1, where only the most vulnerable buildings are updated, minimal impact on the FVI is observed. Rather for adaptation scenario 2, where more buildings are retrofitted,

TABLE 6 Flood mitigation analysis parameter updates.

| Parameter	Adaptation scenario 1			Adaptation scenario 2		
	Original class	Updated class	No. of buildings updated	Original class	Updated class	No. of buildings updated
S1: State of conservation	D	A	13	D, C	A	45
S3: Finishing material of the facades	D	B	1	D, C	A	51
S4: Type and condition of frames	D	C	6	D, C	A	281
S5: Openings at the ground floor	D	C	130	D, C	B	501
E2: Concavity and permeability	D	C	22	D, C	B	257
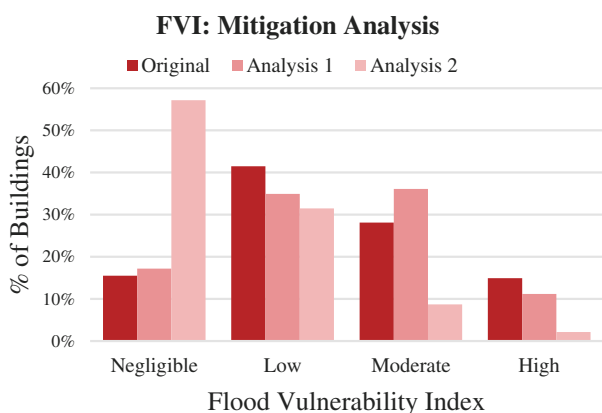
FIGURE 13 Flood vulnerability index comparison for all parameters. Original level.

the FVI shifts left, and a great impact on the flood vulnerability is observed. Figure 14 confirms the decrease in flood risk with building retrofit, improving slightly with adaptation scenario 1 and greatly with adaptation scenario 2. In addition to the graphs, the distribution of buildings impacted by the risk mitigation measures can be seen in the maps below, given in Figures 15–17.

In each series of maps, it is possible to appreciate that the level of flood risk decreases as the updates are made. As is noticeable from these results, the adoption of rehabilitation strategies targeting the characteristics of the buildings that rule their vulnerability to flood can contribute to reducing their vulnerability and, in consequence, reducing the amount of damage if a flood occurs.

6.2 | Cost–benefit analysis

The cost estimation of mitigation measures is an important factor, but the data required to do so is not often available, or it is hidden in non-peer-reviewed literature.

This is an issue in many countries, including Portugal. For the analysis carried out in this work, the cost estimation was completed based on the data presented by Keating et al. (2015). In Table 7, the costs are represented for the dry-proofing measures taking into account the risk mitigation analysis that was performed for the historic city centre of Tomar. Each measure corresponds to a certain parameter which was used in the analysis.

The above costs were used to identify the cost of implementing these measures in the historic city centre of Tomar. This was completed using the prices from the UK and is established as a range of values that would be applicable for the retrofitting strategies mentioned in the risk mitigation analyses. The values are shown in Table 8 (assuming for flood up to 1 m depth).

Typical costs of maintenance work used in the UK have assumed a value between 1% and 5% of the purchase cost of measures (Keating et al., 2015). The costs of these measures were applied to the historic city centre of Tomar. In this way, the buildings that, in the previous analysis, were identified with moderate to extreme flood risk were counted, and the applicable retrofit measures were applied. The cost estimation according to this criterion can be seen in Table 9.

Additionally, the cost distribution over the buildings can be seen in Figure 18. In them, both the low and high ranges of the costs are displayed. The maps show discrete values because they are dependent on the type of intervention strategy applied if necessary. Not each building needs each intervention strategy, depending on the original level of vulnerability.

The costs represented in the maps given in Figure 18 show the cost of the retrofit solutions for each building. From this point, a cost–benefit analysis can be completed. The cost of the interventions can be compared to the damage costs factored determined in Section 5. These costs are compared in Table 10.
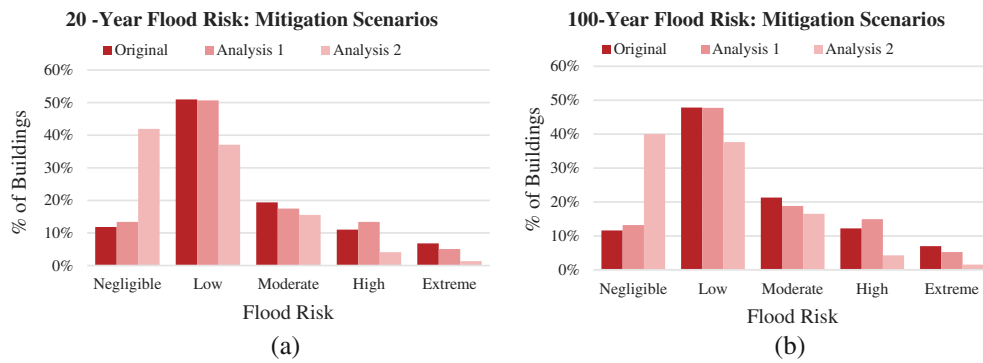
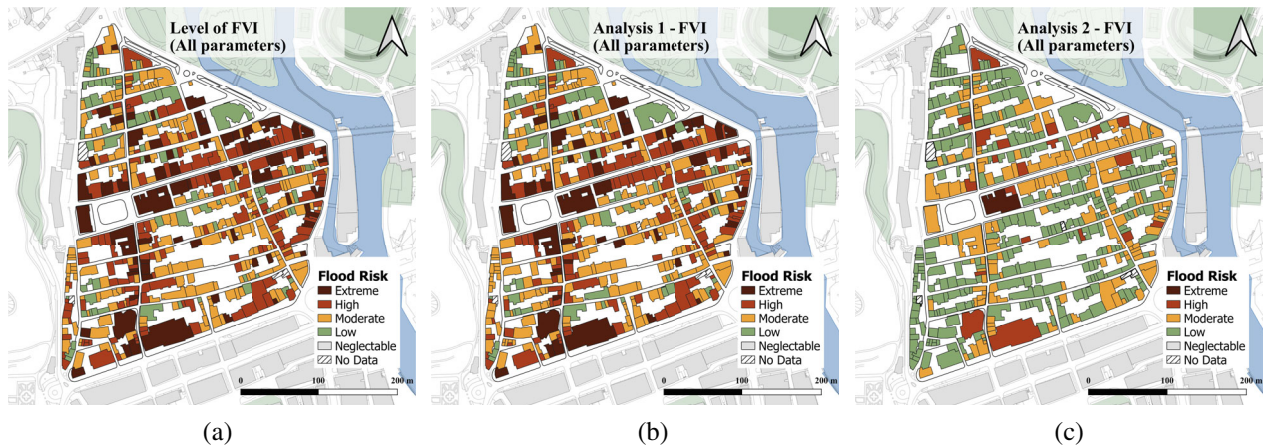**FIGURE 14** (a) Flood risk 20-year and (b) 100-year comparison for all parameters.

FIGURE 15 (a) Original level of flood vulnerability, (b) adaptation scenario 1, (c) adaptation scenario 2.
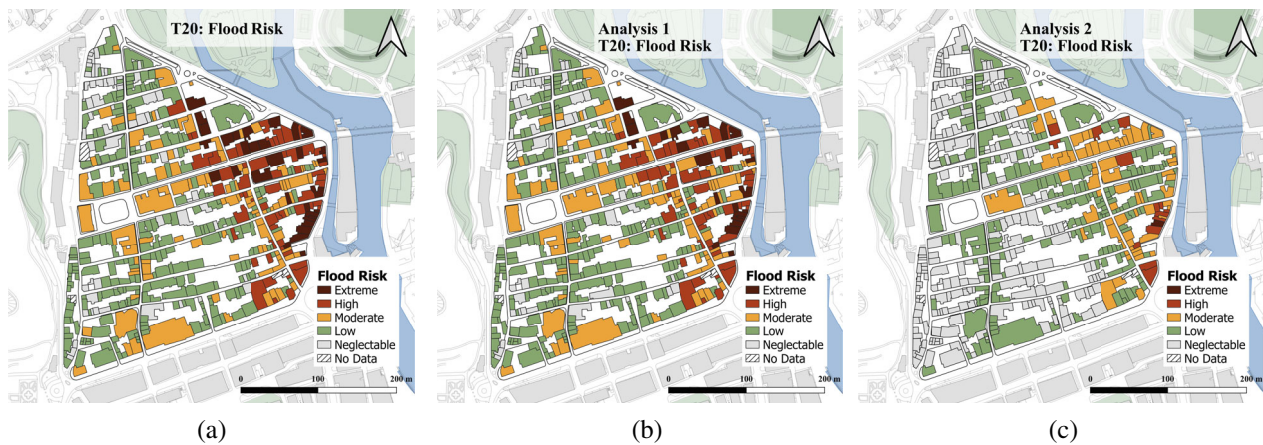

FIGURE 16 (a) Original flood risk 20 year, (b) adaptation scenario 1, (c) adaptation scenario 2.

The cost of the adaptation scenario 1 retrofit is lower than the cost that the damages would incur, showing a positive economic balance. However, the retrofit cost of scenario 2 is higher than the cost of the damages that would incur. In this case, a long-term cost–benefit analysis, including the estimated cost of damage over multiple years and savings due to retrofit efforts, would need to be completed before a recommendation on the amount of retrofit can be completed. This analysis can help with citywide decision-making for phased intervention planning. Phases of retrofitting can be used to first apply these measures to buildings with an extreme level of flood risk, then a high level of flood risk and, finally, buildings with a moderate level of flood risk.

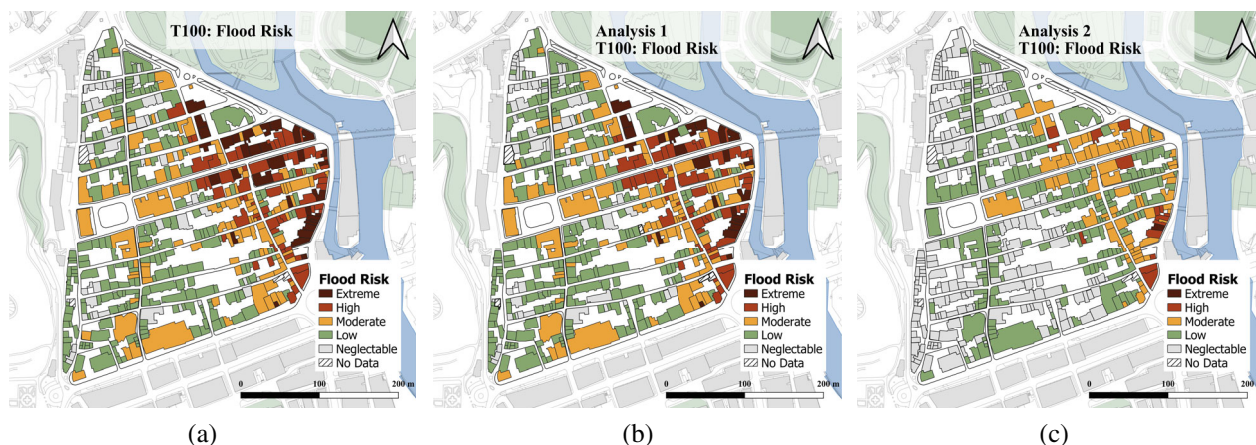By implementing these risk mitigation measures, the flood risk from both the 20- and 100-year floods can be

FIGURE 17 (a) Original flood risk 100 year, (b) adaptation scenario 1, (c) adaptation scenario 2.

TABLE 7 Indicative costs of flood protection measures for the United Kingdom (Keating et al., 2015).

Measure	Parameter	Cost (UK)	Cost (2021, €)	Comments
Additional layer (render, brick, facing) (per m)	S1/S3	£50–100	€58–116	
Flood-resistant door (per door)	S4	£875–2500	€1015.2–2900.5	
Flood skirt (per house)	S3	£10,000–35,000	€11,602.1–40,607.35	Cost includes construction, fitting, and training
Automatic door guard (domestic 2 m opening)	S5	£8000	€9281.7	Costs are inclusive of groundwork and construction

TABLE 8 Cost of replacement with flood resilience alternative assuming flooding up to 1 m in depth. (Keating et al., 2015)

Measure	Parameter	Cost (2003, UK)	Cost (2021, euro)
Coat exterior walls	S1/S3	£2400–8000	€2784.5–9281.7
Flood door, windows, skirting board and frames	S4	£8100–15,000	€9397.7–17,403.15
Repoint brickwork	S1	£3900–12,800	€4524.8–14,850.7

TABLE 9 Cost of adaptations measures 1 and 2.

Parameter	Adaptation scenario 1			Adaptation scenario 2		
	Low (€)	High (€)	# of buildings applied to	Low (€)	High (€)	# of buildings applied to
S1	13,600	44,500	3	95,000	311,900	21
S3	0	0	0	72,400	241,300	26
S5	65,800	1,218,500	70	1,748,000	3,237,000	186
Total	671,400	126,300	73	1,915,400	3,790,200	187

greatly diminished. Specifically, by using flood doors and flood skirts and improving the drainage systems, it is possible to significantly reduce the impact of floods. By implementing these strategies in phases, from the buildings with the highest flood risk to the ones with lower flood risk, the cost of interventions can be distributed first to the buildings that need it the most.

Additionally, implementing flood risk mitigation measures can change the economic damage associated with floods. As introduced in Section 5, the economic damage due to floods can be determined and factored based on the level of flood risk associated with each building and their respective vulnerability. Since the risk mitigation analyses decrease the flood risk associated
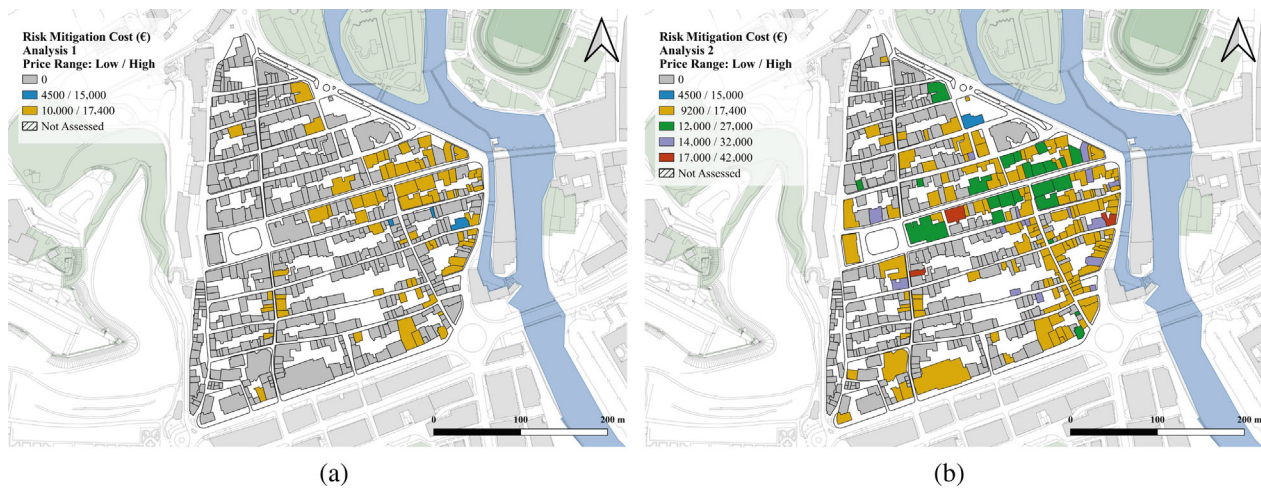
FIGURE 18 Cost of risk mitigation measures: (a) adaptation scenario 1 and (b) adaptation scenario 2.

TABLE 10 Cost associated with depth damage curves as well as mitigation analyses.

Type of cost	Cost (€)
Damage total cost	1,993,000
Analysis 1—Retrofit total cost	126,300
Analysis 2—Retrofit total cost	3,790,200

TABLE 11 Estimation of costs resulting from avoided damages due to the adoption of Adaptation Measures 1 and 2.

Type of damage cost	Cost (€)	% difference from original
Original total damage	1,993,000	
Damage after AM1 retrofit	1,947,500	2%
Damage after AM2 retrofit	1,605,600	22%

with each building, the associated damage cost mitigation can be measured. By recalculating the damage cost associated with each building based on the factored curves from Figure 11, the cost difference for each analysis can be determined, see Table 11.

The differences in cost savings, as a result of avoided damages, can be included in long-term cost–benefit analysis. Additionally, the fact that the mitigations decrease the cost of damage proves the impact of both mitigation measures.

7 | CONCLUSIONS

The type of large-scale vulnerability and risk assessment discussed in this article allows for citywide decision-making, which is crucial for planning phased interventions. Moreover, the mitigation analysis conducted assists in visualising the improvements to the vulnerability of the buildings due to interventions.

The use of cloud-based surveying proved to be a very effective and efficient way of collecting and managing field data. In this specific case, it was possible to conduct a survey of over 500 buildings in 2 days with a team of five surveyors. Although it was not free of technological difficulties—the ability to store the data from multiple devices coming in at the same time was an issue—

overall, it was found that it is an efficient way to collect the necessary data.

In terms of major results, it was possible to observe that most of the buildings identified with higher levels of risk are in the commercial streets perpendicular to the river. This high level of risk is associated with the high vulnerability of buildings themselves, to a great extent, due to their type of use on the ground floor. On the other hand, the high level of risk identified for the buildings located near the river is primarily associated with the high level of hazard in those locations. It is also worthy of note here that most of the buildings located in the centre of the city were identified as having a low level of flood vulnerability. This is further reiterated by the distribution of the flood vulnerability index values, which was skewed to the left. The reason for this low vulnerability is likely due to the low material and structural heterogeneity of the buildings across the city centre.

Throughout this analysis, it was noted that the difference between the 20- and the 100-year return periods was not very significant. Thus, both risk levels showed similar levels of urgency with respect to the need to adopt flood adaptation measures. Mitigation impacts were also assessed in this analysis. It was found that decreasing the

number of openings, installing floodgates, and improving drainage systems have the greatest potential to mitigate flood risk. It was also determined that many buildings needed to be retrofitted to significantly decrease the flood risk throughout the city centre. The costs of these mitigation techniques provide interesting data regarding the potential phases of application, starting from the buildings that are at higher risk and finishing with those that present less risk. The impacts of flooding should be considered on a citywide level. Damages and the cost of mitigation measures should be considered by the government to save lives and mitigate the risks that a flood can cause, in a frequently difficult balance between the effectiveness of those techniques and reglementary and compatibility-related issues.

CONFLICT OF INTEREST STATEMENT
The authors declare no conflicts of interest.

DATA AVAILABILITY STATEMENT
The data that support the findings of this study are available from the corresponding author.

ORCID
Pedro Pinto Santos https://orcid.org/0000-0001-9785-0180
Tiago Miguel Ferreira https://orcid.org/0000-0001-6454-7927

REFERENCES
Arrighi, C. (2021). A global scale analysis of river flood risk of UNESCO world heritage sites. *Frontiers in Water*, *3*(December), 1–12. https://doi.org/10.3389/frwa.2021.764459

Baquedano Juliá, P., & Ferreira, T. M. (2021). From single- to multi-hazard vulnerability and risk in historic urban areas: A literature review. In *Natural Hazards (Issue 0123456789)* (pp. 93–128). Springer. https://doi.org/10.1007/s11069-021-04734-5

Bonazza, A., Maxwell, I., Drdácký, M., Vintzileou, E., & Hanus, C. (2018). *Safeguarding cultural heritage from natural and man-made disasters—A comparative analysis of risk management in the EU*. European Commission. https://publications.europa.eu/en/publication-detail/-/publication/8fe9ea60-4cea-11e8-be1d-01aa75ed71a1/language-en

Brandão, C., Saramago, M. M., Ferreira, T., Cunha, S., Costa, S., Alvarez, T., Carvalho, F. F. d., Silva, M., Duarte, C., Braunschweig, F., Brito, D., Fernandes, L., Jauch, E., & Silva, R. P. (2014). *Elaboração de Cartografia Específica sobre Risco de Inundação para Portugal Continental*. Final Report—Vol. 1: Memória Descritiva. P. 260. Agência Portuguesa do Ambiente.

Câmara Municipal de Tomar. (2021). No title. http://www.cm-tomar.pt/

D'Ayala, D., Wang, K., Yan, Y., Smith, H., Massam, A., Filipova, V., & Jacqueline Pereira, J. (2020). Flood vulnerability and risk assessment of urban traditional buildings in a heritage district of Kuala Lumpur, Malaysia. *Natural Hazards and Earth System Sciences*, *20*(8), 2221–2241. https://doi.org/10.5194/nhess-20-2221-2020

Dutta, D., Herath, S., & Musiake, K. (2001). Direct flood damage modeling towards urban flood risk management. *Joint Workshop on Urban Safety Enginneering*, 127–143.

Fatorić, S., & Seekamp, E. (2017). Are cultural heritage and resources threatened by climate change? A systematic literature review. *Climatic Change*, *142*(1–2), 227–254. https://doi.org/10.1007/s10584-017-1929-9

FBO Consultores. (2003). *Adenda 1. Relatório 1—Análise das cheias na situação actual. Estudo hidrológico e hidráulico no rio Nabão na zona de intervenção do programa POLIS na cidade de Tomar*. TomarPolis.

FEMA. (2008). Flood damage-resistant materials requirements. *Technical Bulletin*. 2, August.

Ferreira, T. M., & Santos, P. P. (2020). An integrated approach for assessing flood risk in historic city centres. *Water*, *12*(6), 1648. https://doi.org/10.3390/w12061648

Gandini, A., Egusquiza, A., Garmendia, L., & San-José, J. T. (2018). Vulnerability assessment of cultural heritage sites towards flooding events. *IOP Conference Series: Materials Science and Engineering*, *364*(1), 012028. https://doi.org/10.1088/1757-899X/364/1/012028

Gandini, A., Garmendia, L., Prieto, I., Álvarez, I., & San-José, J. T. (2020). A holistic and multi-stakeholder methodology for vulnerability assessment of cities to flooding and extreme precipitation events. *Sustainable Cities and Society*, *63*(May), 102437. https://doi.org/10.1016/j.scs.2020.102437

Granda, S., & Ferreira, T. M. (2019). Assessing vulnerability and fire risk in old urban areas: Application to the historical Centre of Guimarães. *Fire Technology*, *55*(1), 105–127. https://doi.org/10.1007/s10694-018-0778-z

Hegger, D., Driessen, P., & Bakker, M. (2016). *A review on more resilient flood risk governance: Key conclusions of the STAR-FLOOD project (D6.4)*. https://www.starflood.eu/documents/2016/03/d6-4-final-report-webversion.pdf/

Historical sales prices Tomar and Santa Maria dos Olivais. (2021). *Idealista*. https://www.idealista.pt/media/relatorios-preco-habitacao/venda/santarem/tomar/tomar-e-santa-maria-dos-olivais/historico/

Holicky, M., & Sykora, M. (2010). Risk assessment of heritage structures endangered by fluvial floods. *WIT Transactions on Ecology and the Environment*, *133*, 205–213. https://doi.org/10.2495/FRIAR100181

Huang, D., Zhang, R., Huo, Z., Mao, F. E. Y., & Zheng, W. (2012). An assessment of multidimensional flood vulnerability at the provincial scale in China based on the DEA method. *Natural Hazards*, *64*(2), 1575–1586. https://doi.org/10.1007/s11069-012-0323-1

Jigyasu, R. (2016). Reducing disaster risks to urban cultural heritage: global challenges and opportunities. *Journal of Heritage Management*, *1*(1), 59–67. https://doi.org/10.1177/2455929616649476

Jigyasu, R., Murthy, M., Boccardi, G., King, J., O'Brien, G., Dolcemascolo, G., Kim, Y., Albrito, P., & Osihn, M. (2013). *Heritage and resilience: Issues and opportunities for reducing disaster risks*. 4th Session of the Global Platform for Disaster Risk Reduction, 19–23 May 2013.

Keating, K., May, P., Pettit, A., & Pickering, R. (2015). *Cost estimation for household flood resistance and resilience measures* (Issue SC080039/R11). https://www.gov.uk/government/uploads/system/uploads/attachment_data/file/411182/Cost_estimation_for_household_flood_resistance_and_resilience_measures.pdf

Lanza, S. G. (2003). Flood hazard threat on cultural heritage in the town of Genoa (Italy). *Journal of Cultural Heritage*, *4*(3), 159–167. https://doi.org/10.1016/S1296-2074(03)00042-6

Martínez-Gomariz, E., Forero-Ortiz, E., Guerrero-Hidalga, M., Castán, S., & Gómez, M. (2020). Flood depth-damage curves for Spanish urban areas. *Sustainability (Switzerland)*, *12*(7), 2666. https://doi.org/10.3390/su12072666

Martínez-Gomariz, E., Forero-Ortiz, E., Russo, B., Locatelli, C., Guerrero-Hidalga, M., Yubero, D., & Castand, S. (2021). A novel expert opinion-based approach to compute estimations of flood damage to property in dense urban environments. Barcelona case study. *Journal of Hydrology*, *598*, 126244. https://doi.org/10.1016/j.jhydrol.2021.126244

Mebarki, A., Valencia, N., Salagnac, J. L., & Barroca, B. (2012). Flood hazards and masonry constructions: A probabilistic framework for damage, risk and resilience at urban scale. *Natural Hazards and Earth System Science*, *12*(5), 1799–1809. https://doi.org/10.5194/nhess-12-1799-2012

Memória Digital de Thomar. (2013). *Máquina do Tempo. Parceria entre Agrupamento Nuno de Santa Maria*. Câmara Municipal de Tomar, Convento de Cristo, Instituto Politécnico de Tomar. http://www.mdthomar.ipt.pt/index.php?pagina=fototeca&categoria=53#

Merz, B., Blöschl, G., Vorogushyn, S., Dottori, F., Aerts, J. C. J. H., Bates, P., Bertola, M., Kemter, M., Kreibich, H., Lall, U., & Macdonald, E. (2021). Causes, impacts and patterns of disastrous river floods. *Nature Reviews Earth and Environment*, *2*(9), 592–609. https://doi.org/10.1038/s43017-021-00195-3

Miranda, F. N., & Ferreira, T. M. (2019). A simplified approach for flood vulnerability assessment of historic sites. *Natural Hazards*, *96*(2), 713–730. https://doi.org/10.1007/s11069-018-03565-1

Nasiri, H., Mohd Yusof, M. J., & Mohammad Ali, T. A. (2016). An overview to flood vulnerability assessment methods. *Sustainable Water Resources Management*, *2*(3), 331–336. https://doi.org/10.1007/s40899-016-0051-x

Rana, I. A., & Routray, J. K. (2016). Actual vis-à-vis perceived risk of flood prone urban communities in Pakistan. *International Journal of Disaster Risk Reduction*, *19*(September), 366–378. https://doi.org/10.1016/j.ijdrr.2016.08.028

Rentschler, J., Salhab, M., & Jafino, B. A. (2022). Flood exposure and poverty in 188 countries. *Nature Communications*, *13*, 3527. https://doi.org/10.1038/s41467-022-30727-4

Rodrigues, S. C. (2017). *Aplicação de metodologias SIG à avaliação da perigosidade de inundação fluvial. O caso da cidade de Tomar*. IPT—Instituto Politécnico de Tomar.

Saisana, M., & Tarantola, S. (2002). *State-of-the-art report on current methodologies and practices for composite indicator development*. Joint Research Centre. Italy: European Commission, July 1–72. https://doi.org/10.13140/RG.2.1.1505.1762

Sesana, E., Gagnon, A. S., Ciantelli, C., Cassar, J. A., & Hughes, J. J. (2021). Climate change impacts on cultural heritage: A literature review. *Wiley Interdisciplinary Reviews: Climate Change*, *12*(4), 1–29. https://doi.org/10.1002/wcc.710

Stephenson, V., & D'Ayala, D. (2014). A new approach to flood vulnerability assessment for historic buildings in England. *Natural Hazards and Earth System Sciences*, *14*(5), 1035–1048. https://doi.org/10.5194/nhess-14-1035-2014

Tyrrel, K. (2019). *Flood mitigation*. National Conference of State Legislatures. https://www.ncsl.org/research/environment-and-natural-resources/flood-mitigation.aspx

UN. (2015). *Sendai framework for disaster risk reduction 2015–2030*.

UN. (2018). *The 2030 agenda and the sustainable development goals an opportunity for Latin America and the Caribbean*.

UNESCO, ICCROM, ICOMOS, & IUCN. (2010). Managing disaster risks for World Heritage. In *Resource manual*. UNESCO World Heritage Centre. https://whc.unesco.org/en/managing-disaster-risks/

UNESCO; UNEP. (2016). *World heritage nations, and tourism in a changing climate*. UNESCO World Heritage Centre. https://whc.unesco.org/en/tourism-climate-change/

UNESCO-WHC. (2008). Policy document on impacts of climate change and world heritage. *BMJ (Clinical Research Ed.)*, *349*, g5945. http://www.ncbi.nlm.nih.gov/pubmed/25276499

UNESCO-WHC. (2021). *Updating of the 2007 policy document on the impacts of climate change on world heritage properties June*. UNESCO World Heritage Centre. https://whc.unesco.org/archive/2021/whc21-44com-7C-en.pdf

Velasco, M., Cabello, À., & Russo, B. (2016). Flood damage assessment in urban areas. Application to the Raval district of Barcelona using synthetic depth damage curves. *Urban Water Journal*, *13*, 426–440. https://doi.org/10.1080/1573062X.2014.994005

Vojinovic, Z., Hammond, M., Golub, D., Hirunsalee, S., Weesakul, S., Meesuk, V., Medina, N., Sanchez, A., Kumara, S., & Abbott, M. (2016). Holistic approach to flood risk assessment in areas with cultural heritage: A practical application in Ayutthaya, Thailand. *Natural Hazards*, *81*(1), 589–616. https://doi.org/10.1007/s11069-015-2098-7

Xiao, S., Li, N., & Guo, X. (2021). Analysis of flood impacts on masonry structures and mitigation measures. *Journal of Flood Risk Management*, *14*(4), e12743. https://doi.org/10.1111/jfr3.12743